

Accuracy Study of a Torsionally Oscillating Pipe Viscometer

S. Clara^{1}, F. Feichtinger¹, T. Voglhuber-Brunnmaier^{1,2}, A.O. Niedermayer¹ und B. Jakoby¹*

¹*Institute for Microelectronics and Microsensors*

²*Linz Institute of Technology*

Altenbergerstr. 69, 4040 Linz, Österreich

Abstract

We recently presented a robust viscosity measurement system based on a torsionally oscillating pipe. This resonant sensor consists of two concentrically aligned pipes. The outer pipe acts as an oscillating torsion spring while the inner one remains at rest. At both ends of the pipe flywheels are located, oscillating against each other in the torsional mode. The pipe is filled with a fluid, which is causing additional damping related to its viscosity. In this contribution we present the sensor setup, describe the measurement principle and analyze the viscosity measurement accuracy achieved in test measurements for different viscous fluids.

Keywords: viscosity, flow-through, resonant, balanced, torsional oscillation.

Introduction

Several resonant viscosity sensors have been presented over the last years, see, e.g., [1] and [2]. Most of these sensors are working in the higher frequency regime above 20 kHz or even in the MHz regime (see [3] and [4]). These high resonance frequencies result in a low penetration depth and therefore a very thin fluid layer being sensed directly on the surface of the sensor which leads to spurious influences due to surface contamination. In this contribution we present an accuracy study of our recently presented viscosity sensor based on a torsionally oscillating pipe [5] and [6] with a low resonance frequency around 7.7 kHz. The sensor setup is almost completely machined in aluminum and is actuated and read out electromagnetically. This relatively large and robust sensor can be used as a flow-through sensor due to its special aligned pipe system.

Setup

The main components of this sensor-system are two concentrically aligned pipes (Figure 1.3 and Figure 1.4) suspended with a mounting spring in the center (Figure 1.2). This mounting spring is located at the position of the nodal point of the torsional oscillation mode, which reduces the influence of the mounting structure on the oscillation drastically. The outer pipe has two flywheels (Figure 1.10) at its ends.

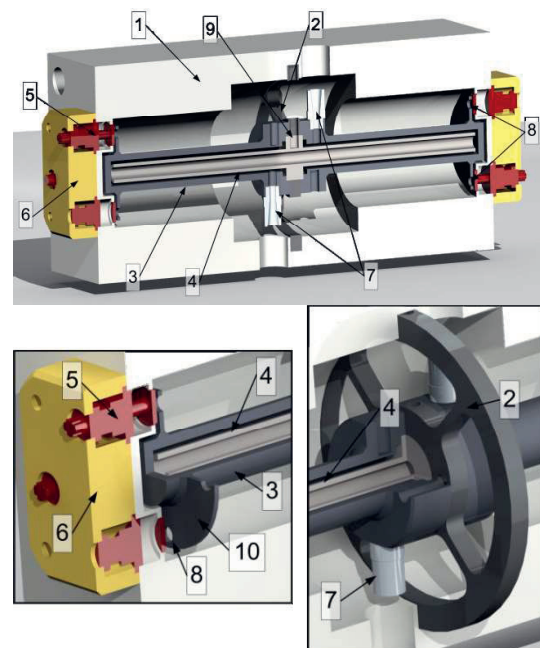


Figure 1: Sensor setup: 1) housing, 2) mounting spring, 3) outer pipe, 4) inner pipe, 5) actuation coils, 6) coil housing, 7) in- outlet, 8) drills for permanent magnets, 9) drill for temperature sensor and 10) fly wheels.

The dimensions of these flywheels combined with the thickness of the outer pipe allow easy control of the resonance frequency of the oscillator (Note: by changing these dimensions also the sensitivity of the sensor is influenced).

Each of these flywheels has four holes (Figure 1.8) fitted with permanent magnets. Next to the permanent magnets, electro-magnetic coils (Figure 1.5) are attached to the sensor housing (Figure 1.1). These coils have an angular offset to the position of the permanent magnets and are used to actuate a torsional oscillation along the outer pipe. If the sensor is filled with a fluid through the two Luer-Lok (Figure 1.7) connectors, placed close to the mounting spring, the periodically moving inner surface of the outer pipe leads to a shear wave traveling into the fluid. Due to this interaction the oscillation of the resonator is damped. This damping is related to the viscosity η and density ρ of the fluid in the sensor. The inner pipe is not oscillating and is only used to guide the fluid through the setup and guarantee homogeneous filling with the fluid. Due to this concentric pipe arrangement, the sensor is also suitable as a flow-through sensor. The whole demonstrator is machined of aluminum except from the in-outlets and the actuation coils. Aluminum was chosen as prototype material due to its low intrinsic damping and its easy machinability.

The housing of the sensor is 70mm x 70mm x 140mm, the outer pipe $D_a = 12\text{mm}$, $D_i = 8\text{mm}$, $L_a = 134\text{mm}$, the inner pipe $d_a = 6\text{mm}$ $d_i = 4\text{mm}$, $l_i = 128\text{mm}$ and the flywheels are $d = 30\text{mm}$ and $h = 1\text{mm}$.

Readout and Actuation

The resonator is actuated using two coils shown in Figure 1.5. Also a four coil actuation, reducing the stimulation of other modes, is possible but not necessary in the present configuration because the resonance frequencies of the different modes are well separated from the resonance frequency of the torsional mode. These coils are opposing the permanent magnets placed in the flywheels (with an angular offset). If the coils are driven accordingly a moment of force is acting on the flywheel on one side of the sensor. In the torsional oscillation mode the second flywheel is rotating against the first one, the outer pipe is twisted, but the center of the pipe, where also the mounting spring is located, represents a nodal point and is ideally not oscillating.

The oscillating flywheel, with the permanent magnets, on the other side is moving in front of the readout-coils inducing a voltage which is proportional to the angular velocity of the flywheel. This signal is used to detect the motion of the flywheel. The polarity of the permanent magnets on the readout side and the connection of the coils are carried out in a way to suppress induced voltages due to the magnetic field of the actuation-coils.

As measurement device for the readout and actuation of the sensor the MFA200 from Microresonant (www.micro-resonant.at) is used. This system stimulates the sensor with eight frequencies simultaneously and measures the response of the sensor [7]. This allows to monitor the quality factor Q and the resonance frequency f_r at a very high repetition rate of around five seconds per sample (also much higher sample rates are possible depending on the quality factor of the resonator). The used frequencies are distributed around the resonance frequency and allow the reconstruction of the frequency response of the sensor.

Modeling

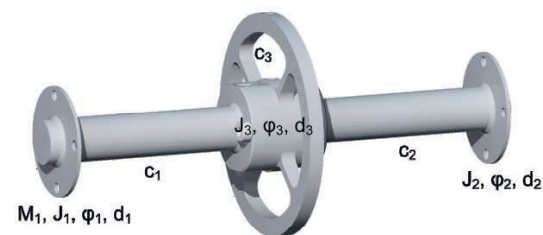


Figure 2: Sketch of a simple 1d model of the mechanical system.

To model the mechanical behavior of the system a simple one dimensional model is sufficient. Figure 2 shows the necessary parameter of a simple 1d mechanical model of the system. This model consists of three flywheels (moments of inertia J_1 , J_2 and J_3), two torsional springs with the spring constants c_1 and c_2 and the mounting spring with the spring constant c_3 . The deflection angles are defined as φ_1 , φ_2 and φ_3 .

The three resonances are clearly visible in Figure 3. The lowest resonance is the symmetric mode. In this mode all three flywheels are oscillating symmetrically against the mounting spring in the middle with the spring constant c_3 . In the mode at 10.2 kHz the outer flywheels oscillate against the one in the middle of the system. The mode used for the viscosity measurements is the mode at 7.7 kHz, in this mode the outer flywheels oscillate against each other. The flywheel in the middle is in the nodal point of the oscillation and is therefore not moving. All measurements were made in this torsional mode.

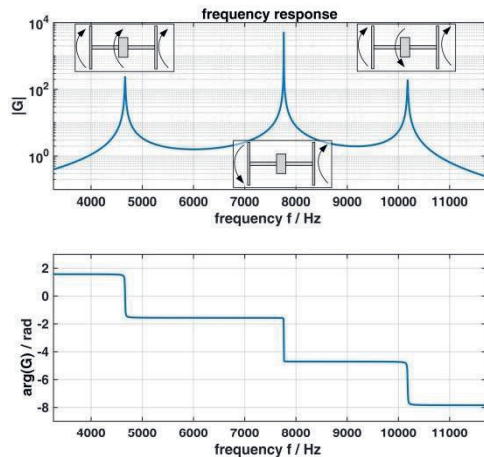


Figure 3: Resonance behavior of the 1d model. The resonance frequencies of the three possible modes are clearly visible. The torsional mode used in the measurements is located in the middle at 7700 Hz.

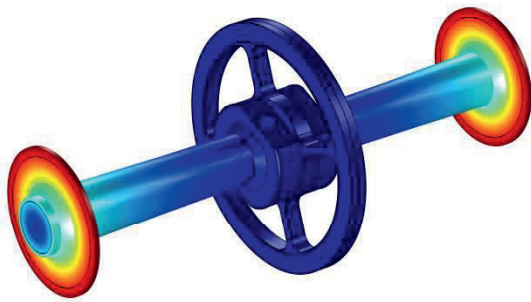


Figure 4: FEM simulation result for the displacement of the mechanical structure oscillating in the torsional mode (red: high deflection, blue low deflection). The resonance frequency of this mode is at 7.7 kHz.

The result of the simple model was validated using COMSOL™ a FEM program, where an eigenmode analyses for the oscillator were performed. Figure 4 shows the result of the FEM simulation of the mechanical structure oscillating in the torsional mode. The increasing deflection along the outer pipe is clearly visible. The mounting spring placed in the middle of the oscillator is not moving. A more complex model including the interaction with the fluid was presented in [6].

Measurement Setup

Different viscosity standard oils were measured at $20 \pm 0.01^\circ\text{C}$ to characterize the sensor setup and study its behavior for high and low viscosities. The used oils are listed in Table 1, the viscosity range is from 19.3 mPa.s

to 7 Pa.s. The range was chosen to provide a large viscosity range but does not represent the limits of the sensor. As shown in [6] also lower viscous fluids with viscosities of 1.96 mPa.s and below are measurable and also higher viscous fluids with viscosities up to 21.5 Pa.s were already measured. The measurements were performed using the MFA200 analyzer from Microresonant (presented in [7] and [8] www.microresonant.at) and an automated sampling system. The whole setup was placed in an isolated temperature box where the temperature was controlled by a water-bath. A calibrated PT100 was used to measure the temperature of the setup; this sensor was placed in a drilling close to the center of the setup (see Figure 1.9). The setup was placed in the temperature box (Figure 5) two hours before the sampling was started to guarantee sufficient thermal settling. As the viscosity is highly temperature dependent a precise defined temperature is required for accurate viscosity measurements, e.g. a change of 0.1°C causes a viscosity change of ca. 0.53% for the standard oil N44 at 20°C . After the temperature settling time a fluid sample was pumped into the sensor and was monitored for one hour. The used measurement system provides one value for the quality factor Q and the resonance frequency f_r every five seconds. After 720 measurements the next sample of the same fluid was pumped into the sensor and the measurements were restarted. For each fluid at least four samples were measured.

To switch to the next fluid the measurement setup was cleaned with cleaning solvent and afterwards flushed with air for two minutes. Due to the flow-through possibility it was not necessary to disassemble the sensor for the cleaning process.

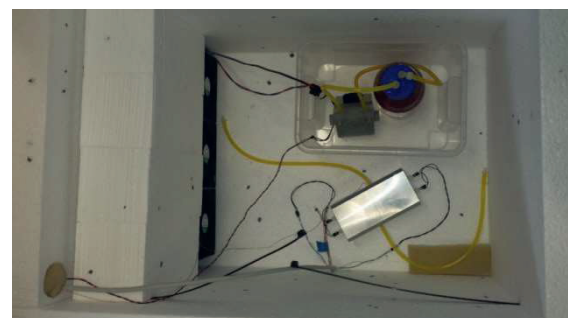


Figure 5: Isolated temperature box containing the viscosity sensor and the automated sampling system (in this picture the sensor is not connected to the sampling system).

Table 1: Viscosity and density values of the measured viscosity standard oils (measured at 20° C).

| Fluids | viscosity η / mPa.s | density ρ / kg / m ³ | damping factor mean(D) | Relative standard deviation $\sigma(D)$ / mean(D) |
|--------|-----------------------------|---|---------------------------|--|
| S2000 | 7000 | 882.8 | 2.500e-03 | 3.138e-02 |
| N415 | 1166 | 845.9 | 1.285e-03 | 1.672e-02 |
| S200 | 602.2 | 887.0 | 9.937e-04 | 1.289e-02 |
| N44 | 91.47 | 827.9 | 4.422e-04 | 5.764e-03 |
| N10 | 19.29 | 870.3 | 2.542e-04 | 7.162e-03 |

Measurement Results

Figure 6 shows a histogram of the measured damping $D=1/2Q$ for N44 at $20\pm0.01^\circ\text{C}$ for all fluid sample measurement points. The mean value is $D=4.422\text{e-}04$ and the standard deviation amounts to 0.5764%.

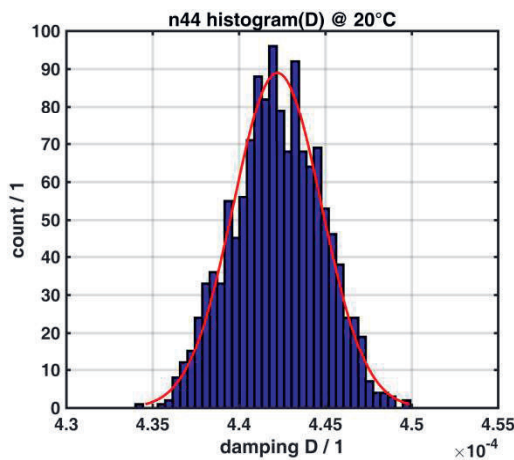


Figure 6: Histogram of the measured damping factor D for N44 at 20 C, for all measured samples.

Figure 7 shows the 3d-histogram where also the temperature is visible. For this diagram only measurements with a temperature in the range of $20\pm0.01^\circ\text{C}$ were considered. This narrow temperature range is necessary due to the strong nonlinear temperature dependency of the viscosity. The temperature is measured as close as possible to the sample, see Figure 1.9.

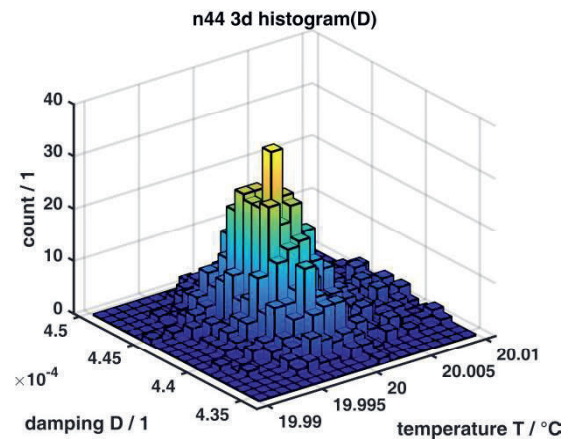


Figure 7: 3d-histogram of the damping factor D and the temperature. To guarantee thermal settling, only temperatures in the range of $20\pm0.01^\circ\text{C}$ are considered.

Figure 8 shows the Damping $D=1/2Q$ versus the $\sqrt{\eta\rho}$. The solid line represents a simple second order polynomial function fitted to the measurement values. It is clearly visible that for low viscosities the damping D is nearly linearly related to $\sqrt{\eta\rho}$. In this region the penetration depth δ (see [9]) of the shear wave is small compared to the fluid layer height ($h_{\eta}=(D_i-d_a)/2=1$ mm) between the outer and the inner pipe. The penetration depth δ is defined as

$$\delta = \sqrt{\frac{2\eta}{\rho\omega}}, \quad (1)$$

where ρ , η and ω denote fluid density, fluid viscosity and angular oscillation frequency, respectively. The linear relation for lower viscosities is not valid for higher viscosities, the penetration depth of the shear wave is for 1 Pa.s in the range of 0.2 mm ($\sqrt{\eta\rho}$ approximately 30), and therefore the influence of the inner pipe is not negligible any more.

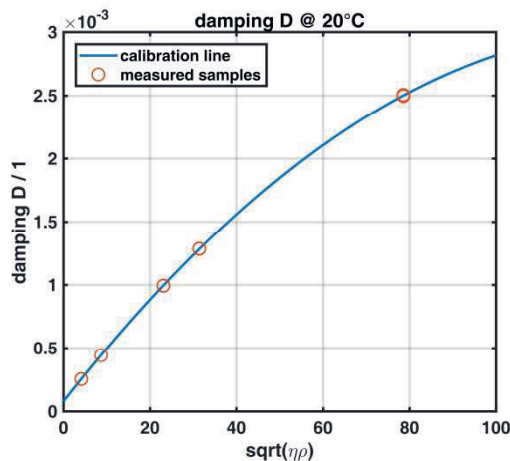


Figure 8: Measured damping D for all measured samples for all fluids versus $\sqrt{\eta\rho}$ calculated from the calibration values of the oils (see Table 1).

Discussion

Figure 9 shows the deviation of the calculated viscosity from the reference viscosity. The blue circles represent the mean value of the calculated viscosity values (calculated from the measured damping factor D for known fluid density ρ), for each sample. For the calculation of the viscosity η the simple polynomial calibration curve, shown in Figure 8, was used. The error for the whole range from 19.3 mPa.s to 7 Pa.s is smaller than 1.5% which, in view of the simplicity of the used model, is a very satisfying result.

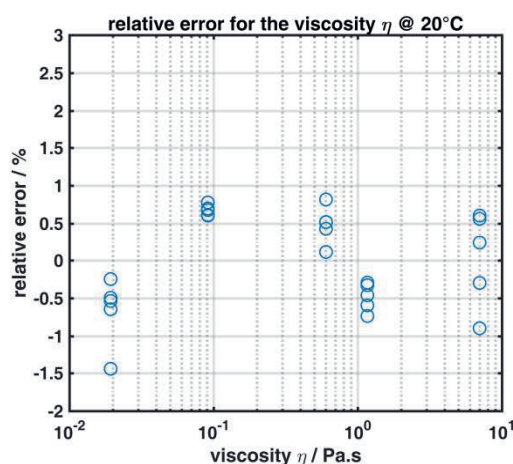


Figure 9: Relative error for the calculated viscosity η for a known density ρ . For the value of the density ρ the nominal values of the calibration oils @ 20°C were used.

Conclusion

We presented a robust viscosity sensor based on a torsionally oscillating pipe. Five different viscosity standard oils were measured at a very well defined temperature of $20 \pm 0.01^\circ\text{C}$. A sampling system was used to automatically change the sample-fluid in the sensor. More than four samples were measured for each standard oil. Each sample was measured for two hours, with a value for the resonance frequency f_r and the quality factor Q every five seconds. A simple second order polynomial calibration curve was used to calibrate the whole measured viscosity range from 19 mPa.s to 7 Pa.s. With this calibration curve the viscosity η was calculated for all measured samples and a relative error of less than 1.5% was achieved. For the calculation the density of the fluid was assumed as known.

Acknowledgments

Financial support was provided by the Austrian research funding association (FFG) under the scope of the COMET programme within the research project "Photonic Sensing for Smarter Processes (PSSP)" (contract # 871974).

References

- [1] B. Jakoby, R. Beigelbeck, F. Keplinger, F. Lucklum, A. Niedermayer, E. K. Reichel, C. Riesch, T. Voglhuber-Brunnmaier and B. Weiss, "Miniaturized sensors for the viscosity and density of liquids-performance and issues," in IEEE Transactions on Ultrasonics, Ferroelectrics, and Frequency Control, vol. 57, no. 1, pp. 111-120, Jan. 2010, doi: 10.1109/TUFFC.2010.1386
- [2] S. J. Martin, Victoria Edwards, Granstaff, and Gregory C. Frye, "Characterization of a quartz crystal microbalance with simultaneous mass and liquid loading", Analytical Chemistry 1991 63 (20), 2272-2281, doi: 10.1021/ac00020a015.
- [3] E. K. Reichel, C. Riesch, F. Keplinger, C. E.A. Kirschhock, B. Jakoby, „Analysis and experimental verification of a metallic suspended plate resonator for viscosity sensing", Sensors and Actuators A: Physical, Volume 162, Issue 2, 2010, Pages 418-424, ISSN 0924-4247, doi: 10.1016/j.sna.2010.02.017.
- [4] A. Rahafrooz, S. Pourkamali, "Characterization of rotational mode disk resonator quality factors in liquid", Frequency Control and the European Frequency and Time Forum (FCS), 2011 Joint Conference of the IEEE International, 2011, doi: 10.1109/FCS.2011.5977863
- [5] S. Clara, H. Antlinger, F. Feichtinger, A. O. Niedermayer, T. Voglhuber-Brunnmaier and B. Jakoby, "A balanced flow-through viscosity sensor based on a torsionally resonating pipe,"

- 2017 IEEE SENSORS, Glasgow, 2017, doi: 10.1109/ICSENS.2017.8234137
- [6] S Clara and F Feichtinger and T Voglhuber-Brunnmaier and A O Niedermayer and A Tröls and B Jakoby, "Balanced torsionally oscillating pipe used as a viscosity sensor", Measurement Science and Technology, 2018, doi: 10.1088/1361-6501/aae755.
- [7] A.O. Niedermayer , T Voglhuber-Brunnmaier, J Sell and B Jakoby, "Methods for the robust measurement of the resonant frequency and quality factor of significantly damped resonating devices", 2012 Meas. Sci. Technol. 23 085107, doi: 10.1088/0957-0233/23/8/085107.
- [8] A.O. Niedermayer, T. Voglhuber-Brunnmaier, M. Heinisch, F. Feichtinger, B. Jakoby, "Monitoring of the Dilution of Motor Oil with Diesel Using an Advanced Resonant Sensor System", Procedia Engineering, Volume 168, 2016, Pages 15-18, ISSN 1877-7058, doi: 10.1016/j.proeng.2016.11.116.
- [9] L.D. Landau, E.M. Lifshitz, "Fluid Mechanics", Butterworth-Heinemann, 1987